Tropospheric ozone over a tropical Atlantic station in the northern hemisphere: Paramaribo, Surinam (6°N, 55°W).

W. Peters*[1], M.C. Krol[1], J.P.F. Fortuin[2], H.M. Kelder[2], A.M. Thompson[3], C.R. Becker[4], J. Lelieveld[5], and P.J. Crutzen[5]

[1]Institute for Marine and Atmospheric Research Utrecht , P.O. Box 80005, 3508 TA Utrecht, Netherlands
[2]Koninklijke Nederlandse Meteorologische Dienst, P.O. Box 201, 3730 AE De Bilt, Netherlands
[3]Goddard Space Flight Center, NASA, Greenbelt, Maryland 20771, USA
[4]Meteorologische Dienst Suriname, Magnesiumstraat 41, Paramaribo, Suriname
[5]Max Planck Institut für Chemie, P.O.Box 3060, Mainz, D-55128, Germany

Manuscript submitted to

Tellus B

February 4, 2003

Send proofs to:
W. Peters, IMAU, P.O.Box 80005, NL-3508TA, Utrecht, Netherlands

Abstract

We present an analysis of 2.5 years of weekly ozone soundings conducted at a new monitoring station in Paramaribo, Surinam (6°N,55°W). This is currently one of only three ozone sounding stations in the northern hemisphere (NH) tropics, and the only one in the equatorial Atlantic region. Paramaribo is part of the Southern Hemisphere ADditional OZone Sounding program (SHADOZ). Due to its position close to the equator, the Inter Tropical Convergence Zone (ITCZ) passes over Paramaribo twice per year, which results in a semi-annual seasonality of many parameters including relative humidity and ozone. The dataset from Paramaribo is used to (1) evaluate ozone variability relative to precipitation, atmospheric circulation patterns and biomass burning; (2) contrast ozone at the NH equatorial Atlantic with that at nearby southern hemisphere (SH) stations Natal (6°S,35°W) and Ascension (8°S,14°W), (3) compare the seasonality of tropospheric ozone with a satellite-derived ozone product: Tropical Tropospheric Ozone Columns from the Modified Residual method (MR-TTOC). We find that Paramaribo is a distinctly Atlantic station. Despite its position north of the equator, it resembles nearby SH stations during most of the year. Transport patterns in the lower and middle troposphere during February and March differ from SH stations, which leads to a seasonality of ozone with two maxima. MR-TTOC over Paramaribo does not match the observed seasonality of ozone due to the use of a SH ozone sonde climatology in the MR method. The Paramaribo ozone record is used to suggest an improvement for northern hemisphere MR-TTOC retrievals. We conclude that station Paramaribo shows unique features in the region, and clearly adds new information to the existing SHADOZ record.

* *Correspondence to:* W. Peters (W.Peters@phys.uu.nl)

1 Introduction

Tropospheric ozone is measured world-wide since it is important for the oxidation power of the atmosphere, as an air pollutant, and a greenhouse gas (Thompson, 1992; Lelieveld and Dentener, 2000). Data from ozone sounding stations around the world is managed and stored by the World Meteorological Organization (WMO), and most is available through the internet (see *http://www.msc-smc.ec.gc.ca/woudc/index.html*). Although currently close to 30 ozone stations report year-round ozone sounding data to WMO, the spatial coverage of the network is quite poor. The northern hemisphere (NH) is more densely covered than the southern hemisphere (SH), and as few as 10 stations are operated in the 'inner' tropics (10S-10N). Most of these stations are part of the SHADOZ program (Thompson et al., 2003a) started by NASA in 1998 specifically to increase the number of tropical monitoring stations.

Although the SHADOZ project has provided more than 1500 soundings in the SH tropics since 1997, ozone measurements in the NH tropics are still limited. Ozone sounding stations have operated since 1992 in Kuala Lumpur, Malaysia (3°N, 101°E) (Yonemura et al., 2002a) and on a bi-monthly basis in Singapore (1°N, 103°E) (Yonemura et al., 2002b) since 1996. A long-term record exists at Hilo, Hawaii (19°N, 155°W) (Oltmans et al., 1996), Trivandrum, India (8°N, 77°E), and Logan (1999) reports some measurements from Panama (9°N, 80°W), dating back to the 1960's and 70's. This lack of data seriously complicates attempts to establish a global climatology of ozone, and to derive trends for the NH tropical region.

Measurements from stations Natal (6°S,35°W) and Ascension (8°S,14°W) have shown that two processes dominate the seasonal cycle of tropospheric ozone in the equatorial Atlantic region: (1) the annual migration of the ITCZ bringing alternate wet and dry seasons, and (2) photo-chemical production of ozone from biomass burning and lightning activity (Thompson et al., 2003b). The former influences the vertical redistribution of ozone through convection and subsidence, while the latter introduces vertical layers with strongly enhanced ozone volume mixing ratios (VMRs). Natal and Ascension are located several degrees south of the equator and convective overturning of the troposphere roughly dominates the first half of the year (Dec-June), while strong subsidence, biomass burning and lightning typically occur during the second half of the year (July-Nov). Ex-

tensive measurements during TRACE-A (Jacob, 1996; Thompson et al., 1996; Mauzerall et al., 1998) have established a similar picture for most of the SH Atlantic basin.

Does the NH Atlantic region show the same features? Based on the migration of the ITCZ, a different convective signal would be expected, as well as stronger transport of air from (polluted) NH source regions. Moreover, biomass burning may not have a similarly large influence, nor peak in the same months as in the SH. No systematic observations were available to test these hypotheses. The only prolonged ozone record in the NH equatorial region is that of Tropical Tropospheric Ozone Columns (TTOC) retrieved from the Total Ozone Mapping Spectrometer (TOMS) (McPeters and Labow, 1996), obtained from cloud differential (CCD) and cloud slicing techniques (Ziemke et al., 1998; Chandra et al., 1998; Ziemke et al., 2000), or by a Modified-Residual (MR) technique (Fishman et al., 1990; Kim et al., 1996; Hudson and Thompson, 1998; Thompson et al., 2000). These latter observations were shown to be consistent with sondes and *in situ* measurements in the SH (Thompson et al., 2003b), but show remarkably high MR-TTOC in the NH eastern equatorial Atlantic. The following important questions are thus associated with the ozone observations in the NH equatorial region: (1) Is there a strong contrast between the NH Atlantic region and stations south of the equator and if so, what causes these contrasts? (2) Do satellite observations of TTOC with the MR-method capture the seasonality of ozone over the NH tropics accurately? These questions can only be answered through independent measurements from a station in the area.

In September 1999, an ozone sounding station was established in Paramaribo, Surinam (6°N, 55°W). This station is currently the third measurement station in the northern hemisphere tropics with a regular (weekly) ozone sounding program, and the only one in the equatorial Atlantic region. In addition to the combined radio- and ozone sonde program, the station is equipped with a Brewer ozone spectrophotometer that continuously measures UV irradiances, ozone column values, and twice daily stratospheric (Umkehr) ozone profiles. The sonde record also includes measurements of wind, humidity, and temperature.

We present and analyze the ozone measurements from Paramaribo, attempting to answer the questions stated above. Our analysis therefore focuses on the seasonality of ozone in the troposphere, as influenced by transport and photo-chemistry in the NH equatorial area. After describing

measurement procedures at Paramaribo and the data processing in this work (Section 2), we will briefly describe the geographical location of Paramaribo in relation to the position of the other SHADOZ stations, and to the ITCZ (Section 3). Using ozone and relative humidity data, Paramaribo will be contrasted with the SH stations Natal and Ascension during the unique short dry season (Section 4.1), while it will be shown that conditions during NH summer are very comparable to those observed over the SH Atlantic (Section 4.2). This includes the possibility of photo-chemical pollution from biomass burning. Integrated tropospheric ozone columns will be used to show that satellite retrieval of MR-TTOC is not optimal for station Paramaribo (Section 5), and likely not for many locations in the NH tropics. The results are summarized and conclusions presented in Section 6.

2 Methods

Station Paramaribo uses Vaisala RS80-15 radio sondes with a Science Pump electrochemical concentration cell (ECC 6A) sensor for ozone measurements and a HumiCap humidity sensor (Komhyr, 1986) for moisture measurements. Location and wind speed are obtained from GPS navigation on the balloons. The ECC sensor is based on a reduction-oxidation reaction of ambient, ozone containing air with a 1.0% buffered potassium-iodide (KI) solution at a platinum anode. Simultaneous measurements with a Brewer spectrophotometer at the station show that the accuracy of sonde integrated total ozone is 2-5%. Operating procedures and instrument preparation is the same as in other tropical stations in the SHADOZ project, for which estimated precision of total ozone is 5% (Thompson et al., 2003a), and tropospheric accuracy 2-3% (Johnson et al., 2002).

2.1 Data preparation

In this work, data from the period September 1999 to January 2003 is used. Ozone sonde quality is based on criteria set by WMO (WMO, 1995), and is calculated from a comparison of the integrated measured ozone profile to an independent measure for the total ozone column. At Paramaribo, this independent ozone column measurement is provided by direct sun observations from the station's

Brewer spectrophotometer. An ozone profile obtained from a successful Brewer umkehr observation, or from the ozone climatology of Fortuin and Kelder (1998) is appended to the measured profile above the burst level to obtain a complete ozone profile, that is subsequently integrated and compared to the independent value. The resulting correction factor is typically close to 1.0 for ECC sondes (Logan, 1985, 1994). Sondes with a correction factor between 0.8 and 1.2 are accepted for the WMO database. Note that these correction factors are only calculated as diagnostic, and the data presented here is not adjusted base on these correction factors.

Station Paramaribo has an excellent track record of correction factors, as 91% (122 out of 133) of the launches between September 1999 and March 2002 (the period for which correction factors were analyzed) meet the WMO criteria. Most of the sondes that did not meet the criteria suffered from a burst at altitudes far below the ozone maximum. This causes an underestimate of the stratospheric ozone abundance above the burst height, which is used to determine the correction factor. Since the tropospheric data from these profiles was often not affected, 9 of these 11 sondes were included in our analysis after visual inspection, yielding a total of 168 (131+37 after March 2002) sondes for the analysis. Launching of ozone sondes normally occurs at 13:00 UTC (08:00 LT), with a few early or late exceptions. **Paul Fortuin: Can we get correction factors for March 2002-now easily??)**

To facilitate the analysis, each profile was averaged to vertical bins of 0.25km. Standard deviations of the averaged ozone mixing ratios within these bins were within 10% of the mean for 92.5% of the points, indicating that the averages accurately represent their altitude bin. Near the tropopause, this criterion was not always met since the ozone gradients there can be large, even on a 0.25 km scale. Additionally, seasonal averages were constructed through averaging multiple gridded profiles within a calendar month. Logan (1999) determined that in the tropics, a minimum of 20 sondes is required to obtain a standard error (defined as $\sigma/\sqrt{N}$, with N the number of observations and σ the square root of the sample variance) within 7.5% of the mean, with a 95% confidence interval. In our analysis, the number of soundings per month ranged from 11-19, and the calculated standard errors are only within 12% of the mean (with a 95% confidence interval). This shows that the seasonal cycles presented here are significantly influenced by interannual, and inter-monthly variations, and should not be interpreted as long-term averages.

The calculation of the tropopause is based on the temperature lapse rate, using a definition similar to Craig (1965). We defined the tropopause as the level between 9 and 19 km altitude where the temperature lapse rate first exceeds 2K/km, and the ozone mixing ratio does not exceed 150 ppbv. Due to the sharp temperature change near the tropical tropopause, this criterion was easily checked visually, and no data was rejected though this procedure. We also calculated the chemical tropopause, defined as the level where the ozone mixing ratio equals 100 ppbv. On average, the thermal tropopause was 0.71 km higher than the chemical tropopause, and the difference maximized during the dry season (August-November), when enhanced ozone mixing ratios in the upper troposphere lower the 100 ppbv level. For a further analysis of tropopause heights, structure, and variability we refer to *J. P. F. Fortuin, H. M. Kelder and C. R. Becker, Evidence of inertial unstable flow over Suriname during the South American monsoon period, manuscript in preparation, 2003.*

2.2 Air mass origin

To discern the most probable origin of the air masses sampled over Paramaribo, trajectories were calculated for each time a balloon was launched. The trajectories were initialized at pressure levels 900, 800, 700, 600, 500, 400, 300, 200, 150, and 100 hPa, and calculated backwards for five days using a trajectory model based on ECMWF analyzed wind data. Brief quality assessments of ECMWF based trajectories can be found in Pickering et al. (1996); Fuelberg et al. (1996) and Stohl and Koffi (1998).

We recognize the limited applicability of single trajectories in the tropics, due to the strong vertical motions and the role of diabatic processes, especially in the wet season. Moreover, five day backward trajectories from Paramaribo usually originate from the Atlantic Ocean, which complicates attribution of specific ozone features to its sources and sinks. Therefore, we applied some additional modeling techniques, focusing on the possible role of biomass burning emissions on the measured profiles.

In Section 4.2, we use plumes of a modeled tracer to illustrate transport patterns during the long dry season. These plumes were calculated using a global three-dimensional transport model, described in Krol et al. (2001). This model calculates transport of an idealized tracer by advection and convection using the same meteorological information from the ECMWF data that was used to

calculate the trajectories. The transport model employs a coarse geographical resolution of $9° \times 6°$ (lon$\times$lat) in the extra-tropics, a finer $3° \times 2°$ resolution in the tropics, and finest $1° \times 1°$ resolution over the northern part of South America. This is done following a new algorithm that allows on-line, two-way communication between the grids (e.g. two-way nesting). Thus, the detail of information on the finest grid is optimally exploited in the transport simulations. The idealized tracer has a lifetime of one week near the surface, and a lifetime that varies with altitude proportional to the abundance of water vapor. Thus, the lifetime of the tracer increases to four weeks when the water vapor abundance is four times smaller than at the surface. The tracer is released throughout the boundary layer at the time and location where large fires were observed with the Along Track Scanning Radiometer (ATSR) instrument (Arino and Melinotte, 1995) (world fire atlas http://shark1.esrin.esa.it/ionia/FIRE/). In the ATSR algorithm, only nighttime observations in the 3.7 μm channel are used to detect hot spots with temperatures exceeding 600K (Arino and Melinotte, 1998). The simulation is done for the period July 15th through August 30th, and starts with zero concentrations everywhere. This approach was chosen as a simple, qualitative alternative to trajectory calculations. Quantitative modeling of the Paramaribo profiles should be performed using a CTM with full chemistry, including a more detailed description of sources and sinks (Peters et al., 2002).

3 Regional perspective

The most prominent feature determining the seasons in Surinam is the ITCZ. Studies of the ITCZ migration in the vicinity of Surinam have been carried out as part of the GATE experiment (Frank, 1983), circulation and climate studies of South America (Hastenrath, 1966, 1977, 1997, 2000) and our current measurement program (Fortuin et al., 2002).

A first distinction that can be made, based on the position of the ITCZ, is between the wet and dry season. The dry season (August-November) corresponds roughly to the period when the ITCZ is located over the northern equatorial Atlantic (Hastenrath, 1997), north of Paramaribo. The wet season (Dec-July) corresponds to the period when the ITCZ travels from this position southward and back, bringing it over Paramaribo twice. Convection and rain are abundant during the wet

season, which can be viewed as a period with monsoon-like flow, by way of northeasterly inflow of air with the trade winds and southwesterly return flow at higher altitudes ($\sim$ 9-12km), which constitutes the northerly upper branch of the Hadley circulation.

During a short period in February and March, the ITCZ is at its southernmost position, and convection and precipitation over Paramaribo are suppressed by subsidence on the equatorward flank of the North Atlantic high (Hastenrath, 2000). This period is called the short dry season, during which the station is part of the meteorological northern hemisphere. The short dry season divides the wet season in two parts, one in which the ITCZ approaches from the north (Dec-Jan) and one in which the ITCZ approaches from the south (April-July). This latter period lasts longer, and has more intense convection than the former because low level convergence and moisture advection are stronger toward NH spring, when the North Atlantic high intensifies (Snow, 1976) and the northeasterly trade winds are stronger to compensate the strong downward motions.

Figure 1 shows the location of stations Paramaribo, Natal, Ascension, and San Cristobal, as well as the seasonality of rainfall at each station. Clearly, the two continental stations Natal and Paramaribo receive much more rainfall than the two maritime stations Ascension and San Cristobal. As expected, the stations in the SH experience their maximum in rainfall earlier (March-April) than Paramaribo (May-June). Moreover, Paramaribo shows a clear double seasonality of rainfall, with maxima in Dec-Jan and May-June, whereas Natal shows a single, prolonged peak of rainfall from March-July. The other two stations receive little rainfall so that the seasonality is difficult to relate to the passage of the ITCZ.

The influence of the migrating ITCZ on the ozone concentration can clearly be distinguished for Paramaribo (Figure 2). The most prominent features are the lower ozone concentrations ($<$ 40 ppbv) during the local wet season, which often penetrate to over 12 km altitude. This occurs predominantly in the months between April and July, but there are occurrences in other months (for instance on 22/03/2000, 19/12/2001, 30/10/2002) showing that the ITCZ is not the only factor determining the stability of the atmosphere over Paramaribo. The ITCZ is positioned directly over the station in late May and June and mixes low ozone VMRs throughout the altitudes between 3-12 km. In April and July, the ITCZ is located further away from Paramaribo and localized minima of ozone that was advected following convection elsewhere can be seen around 10km altitude (Figure

2b, and for instance profiles on 12/04/2000, 15/07/2000, 18/07/2001).

The following long dry season is characterized by much higher ozone mixing ratios, especially in the middle and upper troposphere. This is very similar to the other SHADOZ stations, of which the tropospheric ozone seasonality is depicted in Figure 3, suggesting that similar processes (subsidence, biomass burning, lightning NO_x) influence ozone here. As hypothesized, the influence is smaller than at the SH stations, as absolute values of ozone are generally highest at Ascension, lowest at San Cristobal, and higher at Natal than at Paramaribo. For instance, peak values of ozone at Paramaribo never exceed 100 ppbv (averaged over 0.25km bins) below 8 km, and rarely below 13 km altitude, whereas this occurs frequently at both Natal and Ascension (Logan and Kirchhoff, 1986; Thompson et al., 2003a). Generally, Paramaribo also receives much more rain fall during the long dry season (90mm) than Natal (40mm) indicating that the atmosphere is disturbed more frequently.

The short dry season that is obvious in the rainfall statistics of Figure 1, is less prominent in ozone. Nevertheless, each year shows signs of a temporary return to higher ozone VMR's in the first part of the year, dividing the wet season period from December-July in two. The timing and intensity of the short dry season vary strongly though from one year to the next, and this period would not be identified easily from Figure 2a. However, a small effect of increased ozone mixing ratios in the middle free troposphere is visible in the seasonality plot of Figure 2b. In contrast to the same period in other stations in Figure 3, the gradient of ozone increases throughout the free troposphere, without local maxima or minima.

Figure 2a also shows some of the interannual variability in tropospheric ozone which is related to transport. The 2001 short dry season started early, and was stronger than usual. The following wet season was shorter than the year before, while the long dry season was more unstable than for instance in 2002, reflected in ozone VMR's that are relatively low in the lower 4 km.

From a first glance at the seasonality of ozone at a NH Atlantic station, we can thus confirm that convective overturning in the ITCZ indeed introduces contrasts between NH and SH stations during the first half of the year, and that the processes that enhance ozone on the SH during the latter half of the year appear to affect Paramaribo as well. However, we cannot distinguish a 'strong contrast' (Section 1) with the SH stations, as the patterns in Figure 2b and Figure3 resemble each

other quite closely. To see which processes cause the observed differences and similarities, we will analyze the sonde record in more detail for each season separately.

4 Wet and dry seasons

Figure 4a,b,c show vertical profiles of RH and ozone typical of wet season (N=13), short dry season (N=11), and long dry season (N=19) conditions. These profiles belong to a selected month in each season (based on the rain fall in each year and the variability in the profiles) that was chosen to represent its respective seasons most accurately. Thus, sondes from the month of June were chosen to represent wet season conditions, from February to represent short dry season conditions, and sondes from September to represent long dry season conditions. By selecting the typical months, we are better able to illustrate differences between the seasons, while excluding the effects of early and late onset of the seasons from year-to-year. The average profile of all sondes for these months is shown as a bold line.

Looking at the RH profiles, convective moisture transport to the upper troposphere can be recognized during the wet season by values of RH exceeding 40% even at 10 km altitude. Subsidence during the short dry season dries the free troposphere above 3 km altitude, an effect that can also be seen during the long dry season although less strongly. While the latter was reported for much of the SH Atlantic region (Krishnamurti et al., 1993), the former period of intense subsidence is unique to the NH Atlantic region and thus station Paramaribo at this time of year.

Although the ozone mixing ratios clearly minimize ($<$ 40 ppbv below 12 km) during the wet season, the mixing ratios are still high compared to measurements from Pacific stations during convective conditions. For instance, Pacific SHADOZ stations San Cristóbal (see Figure 3c) and Fiji often record ozone mixing ratios below 20 ppbv during the wet seasons, and integrated tropospheric ozone rarely exceeds 20 DU (Thompson et al., 2003a). The VMRs found over Paramaribo are comparable to those at Natal (Figure 3a and (Thompson et al., 2003a)) during the wet season. This could be expected, because both are coastal stations and influenced by easterly surface winds bringing marine air from the Atlantic. Since this region shows higher ozone VMRs than found over the Pacific all year round (Fishman et al., 1990; Thompson et al., 2003a), background values

of ozone are higher in Paramaribo and Natal than over typical Pacific stations, even during wet season convective conditions.

VMRs during the short dry season are clearly much higher than during the wet season, but somewhat lower than during the long dry season, especially between 7-12 km altitude. There, the long dry season shows average ozone values exceeding 60 $\pm$ 25 ppbv, which is introduced through the averaging of many more spatially confined peaks at different altitudes in the individual profiles. This is illustrated by the large variability in the individual profiles, that often have peak values exceeding 80-100 ppbv, as well as minimum values below 55 ppbv. In contrast, the average values during the short dry season do not exceed 60 ppbv in the 7-12 km altitude range, and peak ozone values above 90 ppbv are rare. The short dry season is characterized by elevated background ozone and increased VMRs throughout the column, while the long dry season is characterized by many peak values of ozone. This difference between the two dry seasons can be attributed to the underlying processes that cause the enhancements.

4.1 The short dry season (Feb.-March)

Two processes are responsible for the elevated background ozone values during the short dry season, both of which do not occur at stations south of the ITCZ, nor in the other seasons in Paramaribo. (1) air advected from the NH equatorial Atlantic has higher ozone VMRs during the short dry season than during the other seasons, and (2) strong subsidence of air originating from the upper troposphere brings ozone rich air to the middle troposphere over Surinam.

(1) The first feature is evident from trajectory origins and integrated ozone columns from the surface to 4 km. During the short dry season, trajectory origins at the levels 900-800-700-600 hPa levels (N=76) point to the northern Atlantic region around the Cape Verde islands (16N, 24W). This region was the focus of the 1983 GATE experiment (Frank, 1983), and has been traversed by ships, i.e. the R/V Polarstern in 1993 (Weller et al., 1996) and the R/V Ronald H. Brown in March 1999 (Thompson et al., 2000). Based on ozone measurements from the ships, the area between 14N-30N was characterized as a region influenced by NH mid-latitude air of mixed stratosphere-troposphere origins, while the area between the equator and 14N was more tropical in nature and contained many peaks of ozone ($>$ 60 ppbv) in the lower 5km (Figure 1, in Thompson et al.

(2000)).

For trajectories to Paramaribo that originated from this region (68 out of 76), the integrated column ozone abundances in the lower 4 km over Paramaribo are 10.4 $\pm$ 2.1 DU. If we take all trajectories traversing that same region during other seasons (when this region is separated from the NH mid-latitudes by the ITCZ), the integrated column ozone amounts to only 7.9 $\pm$ 1.7 DU. In total, 13 out of 17 sondes during the short dry season have ozone column abundances in the lower 4 km that exceed the average non-short dry season column abundance by more than one-sigma. This supports the view that elevated ozone VMRs from the NH are transported to Surinam in the trade winds from the north Atlantic region. The air mass origins in the meteorological NH are illustrated in Figure 5.

(2) In the middle troposphere, i.e. the region between 4-7 km, air mass origins differ strongly from those in the lower troposphere. This difference in origin is reflected in different ozone VMRs between the two different air masses, but also in a sharp decrease in relative humidity at 4 km altitude (see Figure 4b). Trajectories indicate that dry, ozone rich air originates from the upper troposphere over South America, and even from as far as the Pacific Ocean. It is transported to the middle troposphere over Surinam through subsidence in an area around Puerto Rico and the Lesser Antilles. This subsidence is a consequence of upper tropospheric convergence, induced by divergent outflow from convection near the equator, where sea surface temperatures are enhanced during this time of year (Hastenrath and Lamb, 1977).

Figure 6 shows an example of 13 of such trajectories associated with different launch dates, superimposed on a GOES-8 water vapor satellite image. The dark regions in the satellite picture denote areas where water vapor abundance is low due to downward motions. This large-scale feature is present throughout most of the short dry season. These trajectories undergo rapid downward motion north of Surinam. Similar motions and trajectories are found in other seasons, although they are less frequent, and the downward motions are weaker.

Based on the ozone record alone we cannot distinguish photochemically produced ozone following biomass burning north of the ITCZ from other possible sources of ozone. During the March 1998 LBA-CLAIRE campaign, clear biomass burning signals were encountered only from South American fires (Andreae et al., 2001), but not from African fires. Trajectory analysis (unpublished

data) for this campaign also indicated NH mid-latitude air from the free troposphere to dominate over air masses from the African boundary layer. However, sun-photometer measurements (Formenti et al., 2001) show Saharan dust to be transported across the Atlantic to Paramaribo frequently, leaving open a possible contribution from African biomass burning sources to the enhanced VMR's during the short dry season.

4.2 The long dry season (Aug.-Nov.)

The most obvious reason for the similarity between Paramaribo, Natal and Ascension during the latter half of the year is the fact that all three stations are then part of the southern meteorological hemisphere, and not separated from each other by the ITCZ, which lies well north of Paramaribo. Thus, the same processes (biomass burning, lightning, subsidence) that cause ozone to increase over much of the SH Atlantic basin (Fishman et al., 1990), as well as Ascension (Thompson et al., 2003a) and Natal on the Brazilian coast (Logan and Kirchhoff, 1986), are likely to affect Paramaribo as well. The influence of subsidence during this period was already seen in Figure 4, the influences of biomass burning and lightning depend strongly on transport patterns in the area.

Figure 7 illustrates how African biomass burning products can reach the free troposphere over station Paramaribo. It shows the 10-day averaged wind field at 500 hPa, for the period July 31st-August 9th, 2000. Black dots over Africa indicate the location of intense fires during this period, as observed by both ATSR nighttime detection of fires (Arino and Melinotte, 1995), as well as by observations of burning scars (Pinty et al., 2000) (see insert of Africa). From these locations, a tracer was released into a transport model as described in Section 2.2. The resulting modeled plume shows that biomass burning products are brought into the middle troposphere in a convective system off the coast of Nigeria, and subsequently transported (in 10 days) to Paramaribo by easterly winds over the Atlantic Ocean. Integrating the measured profile of tropospheric ozone at August 9th (not shown here) yields 42 DU of ozone, mostly due to VMRs of 70-100 ppbv between 5 and 10 km. Such enhancements require an average net ozone production ratio of ~3-5 ppbv/day during the 10-day transport from the biomass burning source. This is within the range of estimates from TRACE-A (Thompson et al., 1996; Jacob, 1996; Mauzerall et al., 1998), as well as from modeling studies (Roelofs et al., 1997; Moxim and Levy, 2000). In the days before August 9th,

enhanced ozone was also seen over the equatorial Atlantic in the EP-TOMS TTOC observations and at station Ascension (51 DU at August 4th). These features support the possibility that aged biomass burning effluents from Africa enhanced ozone VMRs over Paramaribo on August 9th. No sondes were released from Natal in this period.

Biomass burning also occurs in South America during the dry season, possibly influencing our sonde record. Figure 8 shows an example of a case where this is likely to have occurred. In the days before August 30th, 2000, three day averaged wind fields at 400 hPa show transport of air around an upper tropospheric ridge (SH anti-cyclone), which advects air from the Pacific Ocean and Central Brazil to station Paramaribo. The location of fires (ATSR) over Brazil is again indicated by black dots. When we release a tracer from these fires, convection lofts it to the 400 hPa level, where ozone VMRs of ~60 ppbv were sampled between 7-12 km at August 30th. The pattern of the tracer shows the advection to our site. As would be expected from the simulation, the measured profile at Natal is not affected (although sampled at August 31st), with only 17 DU of tropospheric ozone.

The situation in Figure 7 occurs most frequently during the long dry season, as the flow pattern shown closely resembles the monthly averaged winds. Therefore, the amount, frequency, and timing of ozone pollution events at Paramaribo depend mostly on the occurrence and intensity of fires over Africa, lofting of the plumes to the free troposphere by convection, and subsequent transport in the tropical easterlies. In contrast, the situation in Figure 8 is much less frequent, and is associated with anomalous southeasterly winds in the free troposphere. Note that the direction of transport (from Africa, westward to South America) is opposite to that of the 'global plume' (Chatfield et al., 2002), which pollutes the Southern Hemisphere (sub)tropics through easterly transport of biomass burning emissions.

As a final check on the similarity between Paramaribo and the SHADOZ stations in the SH during the long dry season, we have placed the September-October-November (SON) data from station Paramaribo into the zonal wave structure deduced in (Thompson et al., 2003b). This zonal wave structure in tropospheric ozone shows a gradient in VMRs with highest values over the Central Atlantic (Ascension, 14°W), decreasing westwards toward Natal (35°W) and San Cristóbal (90°W). A sharp decrease of VMRs can be seen between the latter two stations, separating the

Atlantic region from the Pacific. Paramaribo (55°W) is located exactly in this region with the strongest gradient between these stations. If we would include the SON average profiles from Paramaribo in the zonal wave one structure, the area of relatively high ozone VMRs would extend further westward. The separation between Atlantic and Pacific in the upper troposphere would be defined even more sharply, and placed longitudinally between 55°W and 90°W, i.e., over the western South American continent.

In conclusion, station Paramaribo generally falls within the relatively ozone-rich Atlantic region where the maxima in the zonal wave one pattern occur. Owing to its more remote location relative to the South Atlantic ozone maximum, and the fact that the lower troposphere is always influenced by maritime air masses, ozone VMRs are lower than at Natal, and fresh ($<$ 2 days old) biomass burning pollution is rarely encountered. The fact that the station's position relative to the ITCZ is different from the SHADOZ stations in the southern hemisphere introduces minor differences during the latter half of the year, but large differences during February-March when Paramaribo is north of the ITCZ.

5 Column Integrated ozone

In Figure 9, the seasonality of TTOC as deduced from the 1999-2002 Paramaribo ozone record is shown. Although the monthly averages in different years show considerable interannual variability, a pattern with two maxima during each of the dry seasons is visible in the figure. Typical long wet season TTOC is 20-30 DU, again comparable to that at Natal. During the short wet season, convection penetrates only up to $\sim$7 km and TTOC can be as high as 30 DU. Especially in January 2001, ozone values were anomalously high when, for a short period, dry season conditions occurred very early in the year.

In the same figure, the seasonality of MR-TTOC as calculated from the 1979–1992 NIMBUS–7 TOMS record is shown (dashed line). MR-TTOC underestimates Paramaribo TTOC by 5-10 DU in February and March when the short dry season occurs, while it overestimates Paramaribo TTOC by up to 10 DU from June-September. Moreover, the seasonality of MR-TTOC displays

one minimum during the first half of the year, and one maximum during the second half of the year, where the Paramaribo sonde record has two TTOC maxima.

We have traced back the cause in this discrepancy to one very important parameter used in the MR-method, which is the thickness of the tropospheric ozone column at the dateline: $\Omega_{bck}^{trop}(180°W)$. By lack of suitable data, this background value was assumed to be constant with latitude in the MR-method. This assumption allows the MR-method to separate the TOMS total column ozone observations into a tropospheric and a stratospheric component at each tropical latitude. The different steps and assumptions in this process are described in detail in (Hudson and Thompson, 1998) and (Thompson and Hudson, 1999), here we will show that specifically this assumption introduces discrepancies, which can be improved using the Paramaribo ozone sondes.

Since there are no direct measurements of $\Omega_{bck}^{trop}(180°W)$, its value in the MR-method is derived using a climatological average tropospheric ozone column over the Atlantic Ocean (0°W), based on 1991-1992 ozone sondes from Natal (6°S, 35°W), Ascension (8°S, 14°W), and Brazzaville (4°S, 15°E). This climatology is combined with the gradient of total ozone between the Atlantic (0°W) and the Pacific (180°W) as derived from TOMS total ozone columns, to calculate $\Omega_{bck}^{trop}(180°W)$. Using a 'test' series of 1998-2000 total ozone column data from EP-TOMS, and the seasonality of the sonde climatology at 0°W as described in Hudson and Thompson (1998), we have calculated $\Omega_{bck}^{trop}(180°W)$ for this period as depicted in Figure 10. Clearly, the Ω_{bck}^{trop}(180°W) inherits the SH seasonality present in the ozone sondes, that were all launched in the southern hemisphere.

However, if we substitute the SH ozone sonde climatology with one based on NH station Paramaribo ozone sondes, the seasonality of Ω_{bck}^{trop}(180°W) reverses as can be seen in Figure 10b. Thus, *the seasonality of $\Omega_{bck}^{trop}(180°W)$ needed to optimally retrieve observed ozone values at Paramaribo is opposite to that derived from SH sondes.* Figure 10 shows the difference between the two derived values of Ω_{bck}^{trop}(180°W), as well as the difference between integrated ozone columns from Paramaribo and MR-TTOC from Figure 9. Since discrepancies in Ω_{bck}^{trop}(180°W) translate linearly to differences in MR-TTOC, the reversed seasonality of Ω_{bck}^{trop}(180°W) on the NH explains almost all of the difference in integrated ozone columns.

The contrasting seasonalities of integrated ozone at either side of the equator around the dateline

are introduced by the migration of the ITCZ. In the first months of the year, the ITCZ is in a southerly position, reducing convection at the NH side of the equator, and also allowing relative ozone rich air from more northerly latitudes to influence the region, and increase TTOC. Likewise, the ITCZ takes a more northerly position from July-October, with similar effects on the SH side of the equator. Correcting $\Omega_{bck}^{trop}(180°\text{W})$ for this effect should be relatively straightforward, and we have shown that this can be done using ozone sondes from Paramaribo. Also, chemistry-transport model calculations that reproduce TTOC at remote tropical locations well (Peters et al., 2002) confirm this opposite seasonality. In this respect, we should also mention that new TOMS TTOC algorithms, currently under development, are no longer constrained by southern hemisphere ozone seasonality and are not expected to show the bias explained here.

However, based on our results, it is highly likely that every location on the NH in the existing 1979-1992 MR-TTOC dataset has a bias toward SH ozone values. This bias is expected to increase with distance from the equator, where seasonal cycles become stronger. It would be interesting to better quantify this bias with more observations, but there are no other distinctly NH stations available for this. Nevertheless, our results suggest that station Paramaribo can be used to improve the seasonality of MR-TTOC over the NH, which highlights again the importance of this new station.

6 Conclusions and Summary

The ozone measurements over Paramaribo are largely controlled by meteorological variability, which is strongly linked to the annual migration of the ITCZ. As expected, ozone and relative humidity vary on a semi-annual time scale due to the passage of the ITCZ in May and December. Although the seasonality of ozone at Paramaribo resembles that at SH stations Natal and Ascension, the existence of the short dry season (Feb-March) distinguishes it from all SH stations in the SHADOZ network.

In February and March, the station is part of the northern meteorological hemisphere, and relatively polluted air from the NH Atlantic region and even from NH mid-latitudes is transported into the lower 4 km of the atmosphere. Moreover, downward transport of ozone rich-air occurs on the

equatorward side of the North Atlantic high, which contributes to high ozone VMRs in the middle troposphere during the short dry season.

In the latter half of the year, Paramaribo is typically a SH Atlantic station, and fits well in the zonal wave one structure of tropospheric ozone that displays its strongest maxima in September-October-November. Besides downward transport of dry, ozone-rich air, we have shown that transport of biomass burning products from Africa is a plausible source of ozone in the free troposphere in this latter period. In contrast, transport of biomass burning products from South American sources is less likely to occur given the prevailing winds. Some weather situations can nevertheless occasionally favor this transport, as we have shown in Section 4.2. Based on the Paramaribo sonde record, the division between the Atlantic and Pacific regime in tropospheric ozone (and relative humidity) can be placed west of Paramaribo (55°W), and east of San Cristobal (90°W), making the natural barrier of the Andes mountains the region where the strongest zonal gradients in tropospheric ozone occur.

We have shown that satellite observed tropospheric ozone columns (MR-TTOC) do not reproduce the observed seasonality at Paramaribo correctly. Underestimates occur during the first months of the year, and overestimates during the second half. Analysis suggests that this is due to an assumption on background ozone over the Pacific (180°W) in the MR-method. By lack of suitable data, this background value was derived using SH ozone sondes. The Paramaribo data and chemistry-transport model results suggest that the seasonality of this background value reverses for the NH, and that data from station Paramaribo can be used to improve the MR-retrieval algorithm.

7 Acknowledgments

We would like to thank the ozone station operators in Paramaribo, who have done a superb job in collecting the data presented here, maintaining the instruments, and assuring high data quality. Also, we acknowledge the support and enthusiasm received from the government of Suriname in establishing this site. Part of this analysis was performed during a visit to NASA Goddard Space Flight Center through the University of Maryland -Baltimore county GEST program, whom we

thank for their hospitality. This research was conducted as part of the RADCHiS program financed by the Dutch Research Council (NWO).

References

Andreae, M. O., Artaxo, P., Fischer, H., Freitas, S. R., Gregoire, J. M., Hansel, A., Hoor, P., Kormann, R., Krejci, R., Lange, L., Lelieveld, J., Lindinger, W., Longo, K., Peters, W., de Reus, M., Scheeren, B., Dias, M. A. F. S., Strom, J., van Velthove, P. J. F., Williams, J., 2001. Transport of biomass burning smoke to the upper troposphere by deep convection in the equatorial region. *Geophys. Res. Lett.* **28**, 951–954.

Arino, O., Melinotte, J.-M., 1995. Fire Index Atlas. *Earth Observation Quarterly* **50**.

Arino, O., Melinotte, J. M., 1998. The 1993 African fire map. *Int. J. of Remote Sensing* **19** (11), 2019–2023.

Chandra, S., Ziemke, J. R., Min, W., Read, W. G., 1998. Effects of 1997-1998 El Niño Southern Oscillation on tropospheric ozone and water vapor. *Geophys. Res. Lett.* **25**, 3867–3870.

Chatfield, R. B., Guo, Z., Sachse, G. W., Blake, D., Blake, N., 2002. The Subtropical Global Plume in PEM-T A, PEM-T B, and GASP: How Tropical Emissions Affect the Remote Pacific. *J. Geophys. Res.* **107** (D16), 1–20, DOI2001JD000497.

Craig, R., 1965. The Upper Atmosphere: Meteorology and Physics. Academic, San Diego, Calif., USA.

Fishman, J., Watson, C. E., Larsen, J. C., Logan, J. A., 1990. Distribution of tropospheric ozone determined from satellite data. *J. Geophys. Res.* **95**, 3599–3617.

Formenti, P., Andreae, M. O., Lange, L., Roberts, G., Cafmeyer, J., Rajta, I., Maenhaut, A., Holben, B. N., Artaxo, P., Lelieveld, J., 2001. Saharan dust in Brazil and Suriname during the Large-Scale Biosphere-Atmosphere Experiment in Amazonia (LBA)- Cooperative LBA Regional Experiment (CLAIRE) in March 1998. *J. Geophys. Res.* **106**, 14,914–14,934.

Fortuin, J. P. F., Kelder, H., 1998. An ozone climatology based on ozonesonde and satellite measurements. *J. Geophys. Res.* **103**, 31,709–31,734.

~~Fortuin, J. P. F., Kelder, H. M., Becker, C. R., 2002. Evidence of inertial unstable flow over Suriname during the South American monsoon period. *manuscript in preparation*.~~

Frank, W. M., 1983. The Structure and Energetics of the East Atlantic Intertropical Convergence Zone. *J. Atmos. Sci.* **40**, 1916–1929.

Fuelberg, H. E., Loring, R. O., Watson, M. V., Sinha, M. C., Pickering, K. E., Sachse, A. M. T. G. W., Blake, D. R., Schoeberl, M. R., 1996. TRACE-A trajectory intercomparison 2. Isentropic and kinematic methods. *J. Geophys. Res.* **101**, 23927–23939.

Hastenrath, S., 1966. On general circulation and energy budget in the area of the Central American seas. *J. Atmos. Sci.* **23**, 604–711.

Hastenrath, S., 1977. On the upper-air circulation over the equatorial Americas. *Arch. Meteor. Geophys. Bioklimatol. Serie A.* **25**, 309–321.

Hastenrath, S., 1997. Annual cycle of upper air circulation and convective activity over the tropical Americas. *J. Geophys. Res.* **102**, 4267–4274.

Hastenrath, S., 2000. Interannual and longer-term variability of upper air circulation in the Northeast Brazil-tropical Atlantic sector. *J. Geophys. Res.* **105**, 7327–7335.

Hastenrath, S., Lamb, P., 1977. Climatic Atlas of the Tropical Atlantic and Eastern Pacific Oceans. Univ. of Wisconsin Press, Madison, USA.

Hudson, R. D., Thompson, A. M., 1998. Tropical Tropospheric Ozone from Total Ozone Mapping Spectrometer by a modified residual method. *J. Geophys. Res.* **103**, 22,129–22,145.

Jacob, D. J., 1996. Origin of ozone and NO_x in the tropical troposphere: A photochemical analysis of aircraft observations over the south Atlantic basin. *J. Geophys. Res.* **101**, 24,235–24,250.

Johnson, B. J., Oltmans, S. J., Vömel, H., Smit, H. G. J., Deshler, T., Kroger, C., 2002. Electrochemical concentration cell (ECC) ozonesonde pump efficiency measurements and tests on the sensitivity to ozone of buffered and unbuffered ECC sensor cathode solutions. *J. Geophys. Res.* **107** (D19), 1–18, DOI10.129/2001JD000557.

Kim, J.-H., Hudson, R. D., Thompson, A. M., 1996. A new method of deriving time-averaged tropospheric column ozone over the tropics using Total Ozone Mapping Spectrometer (TOMS) radiances: Intercomparison and analysis using TRACE-A data. *J. Geophys. Res.* **101**, 24,317–24,330.

Komhyr, W. D., 1986. Handbook- Ozone measurements to 40 km altitude with model 4A-ECC-ozone sondes. NOAA Techn. Memorandum ERL ARL-149.

Krishnamurti, T. N., Fuelberg, H. E., Sinha, M. C., Oosterhoff, D., Bensman, E. L., Kumar, V. B., 1993. The meteorological environment of the tropospheric ozone maximum over the tropical South Atlantic. *J. Geophys. Res.* **98**, 10,621–10,641.

Krol, M. C., Peters, W., Berkvens, P. J. F., Botchev, M. A., 2001. A new algorithm for two-way nesting in global models: Principles and Applications. In: Sportisse, B. (Ed.), Proceedings of the 2nd international conference on air pollution modeling and simulation. Springer Geosciences, New York.

Lelieveld, J., Dentener, F. J., 2000. What controls tropospheric ozone? *J. Geophys. Res.* **105**, 3531–3551.

Logan, J. A., 1985. Tropospheric Ozone: Seasonal behavior, trends and anthropogenic influence. *J. Geophys. Res.* **90**, 10,463–10,482.

Logan, J. A., 1994. Trends in the vertical distribution of ozone: An analysis of ozonesonde data. *J. Geophys. Res.* **99**, 25,553–25,585.

Logan, J. A., 1999. An analysis of ozonesonde data for the troposphere: Recommendations for testing 3-D models and development of a gridded climatology for tropospheric ozone. *J. Geophys. Res.* **104**, 16,115–16,149.

Logan, J. A., Kirchhoff, V. W. J. H., 1986. Seasonal variations of tropospheric ozone at Natal, Brazil. *J. Geophys. Res.* **91**, 7875–7882.

Mauzerall, D. L., Logan, J., Jacob, D. J., Anderson, B. E., Brune, Blake, D. R., Talbot, B., Bradshaw, J. D., Heikes, B., Sachse, G. W., 1998. Photochemistry in biomass burning plumes and implications for tropospheric ozone over the tropical South Atlantic. *J. Geophys. Res.* **103**, 8401–8423.

McPeters, R. D., Labow, G. J., 1996. An assessment of the accuracy of 14.5 years of Nimbus TOMS Version 7 ozone data by comparison with the Dobson network. *Geophys. Res. Lett.* **23**, 3695–3698.

Moxim, W. J., Levy, H., 2000. A model analysis of the tropical South Atlantic Ocean tropospheric ozone maximum; The interaction of transport and chemistry. *J. Geophys. Res.* **105**, 17,393–17,415.

Oltmans, S. J., Hoffman, D. J., Lathrop, J. A., Harris, J. M., Komhyr, W. D., Kuniyuki, D., 1996. Tropospheric ozone during Mauna Loa observatory photochemistry experiment 2 compared to long-term measurements from surface and ozonesonde observations. *J. Geoph. Res.* **101** (D9), 14569–14580.

Peters, W., Krol, M. C., Dentener, F. J., Thompson, A. M., Lelieveld, J., 2002. Chemistry-transport modeling of the satellite observed distribution of tropical tropospheric ozone. *Atmos. Chem. Phys.* **2**, 103–120.

Pickering, K. E., Thompson, A. M., McNamara, D. P., Schoeberl, M. R., Fuelberg, H. E., Loring, R. O., Watson, M. V., Fakhruzzaman, K., Bachmeier, A. S., 1996. TRACE-A trajectory intercomparison 1. Effects of different input analyses. *J. Geophys. Res.* **101**, 23909–23925.

Pinty, B., Roveda, F., Verstraete, M. M., Gobron, N., Govaerts, Y., Martonchik, J. V., Diner, D. J., Kahn, R. A., 2000. Surface albedo retrieval from Meteosat, 2. Applications. *J. Geophys. Res.* **105**, 18,114–18,134.

Roelofs, G. J., Lelieveld, J., Smit, H. G. J., Kley, D., 1997. Ozone production and transports in the tropical Atlantic region during the biomass burning season. *J. Geophys. Res.* **102**, 10,637–10,651.

Snow, J. W., 1976. The Climate of Northern South America. In: Landsberg, H. E. (Ed.), World Survey of Climatology, Vol 12. Elsevier Scientific Publ. Amsterdam, Ch. 6, pp. 305–321.

Stohl, A., Koffi, N. E., 1998. Evaluation of trajectories calculated from ECMWF data against constant volume balloon flights during ETEX. *Atmos. Environ.* **32**, 4151–4156.

Thompson, A. M., 1992. The oxidizing capacity of the Earths atmosphere: Probable past and future changes. *Science* **256**, 1157–1165.

Thompson, A. M., Doddridge, B. G., Witte, J. C., Hudson, R. D., Luke, W. T., Johnson, J. E., Johnson, B. J., Oltmans, S. J., Weller, R., 2000. A tropical Atlantic ozone paradox: Shipboard and satellite views of a tropospheric ozone maximum and wave-one in January-February 1999. *Geophys. Res. Lett.* **27**, 3317–3320.

Thompson, A. M., Hudson, R. D., 1999. Tropical tropospheric ozone (TTO) maps from Nimbus 7 and Earth Probe TOMS by the modified-residual method: Evaluation with sondes, ENSO signals, and trends from Atlantic regional time series. *J. Geophys. Res.* **104**, 26,961–26,975.

Thompson, A. M., Pickering, K. E., McNamara, D. P., Schoeberl, M. R., Hudson, R. D., Kim, J. H., Browell, E. V., Kirchhoff, V. W. J. H., Nganga, D., 1996. Where did tropospheric ozone over Southern Africa and the tropical Atlantic come from in October 1992? Insights from TOMS, GTE/TRACE-A, and SAFARI-92. *J. Geophys. Res.* **101**, 24,251–24,278.

Thompson, A. M., Witte, J. C., McPeters, R. D., Oltmans, S. J., Schmidlin, F. J., Logan, J. A., M.Fujiwara, Kirchhoff, V. W. J. H., Posny, F., Coetzee, G. J. R., Hoegger, B., Kawakami, S., Ogawa, T., Johnson, B. J., Vömel, H., Labow, G., 2003a. The 1998-2000 SHADOZ (Southern Hemisphere ADditional OZonesondes) Tropical Ozone Climatology. 1. Comparisons with TOMS and Ground-based Measurements. *J. Geophys. Res.* **108** (D2), doi:10.1029/2001JD000967.

Thompson, A. M., Witte, J. C., Oltmans, S. J., Schmidlin, F. J., Logan, J. A., Fujiwara, M., Kirchhoff, V. W. J. H., Posny, F., Coetzee, G. J. R., Hoegger, B., Kawakami, S., Ogawa, T., Fortuin, J. P. F., Kelder, H. M., 2003b. The 1998–2000 SHADOZ (Southern Hemisphere ADditional OZonesondes) tropical ozone Climatology. 2. Stratospheric and Tropospheric Ozone Variability and the Zonal Wave-One. *J. Geophys. Res.* **108** (D2), 10.1029/2002JD002241.

Weller, J. W., Lilischkis, R., Schrems, O., Neuber, R., Wessel, S., 1996. Vertical ozone distribution in the marine atmosphere over the central Atlantic Ocean (56°S–50°N). *J. Geophys. Res.* **101**, 1387–1399.

WMO, 1995. Scientific assessment of ozone depletion: 1994. World Meteorological Organization, 37th Edition, Geneva, Switzerland.

Yonemura, S., Tsuruta, H., Kawashima, S., Sudo, S., Peng, L. C., Fook, L., , Johar, Z., Hayashi, M., August 2002a. Tropospheric ozone climatology over peninsular Malaysia from 1992 to 1999. *J. Geophys. Res.* **107** (D15), 1–12, DOI 10.1029/2001JD000993.

Yonemura, S., Tsuruta, H., Sudo, S., Peng, L. C., Fook, L., , Johar, Z., 2002b. Annual and El Niño/Southern Oscillation variations in observations of in-situ stratospheric ozone over peninsular Malaysia. *J. Geophys. Res.* **107** (D13), 1–10, DOI 10.1029/2001JD000518.

Ziemke, J. R., Chandra, S., Barthia, P. K., 2000. "Cloud slicing": A new technique to derive upper tropospheric ozone from satellite measurements. *J. Geoph. Res.* **106** (D9), 9853–9868.

Ziemke, J. R., Chandra, S., Bhartia, P.-K., 1998. Two new methods for deriving tropospheric column ozone from TOMS measurements: The assimilated UARS MLS/HALOE and convective-cloud differential techniques. *J. Geophys. Res.* **103**, 22,115–22,128.

Figure Captions

Fig. 1. Location and seasonality (Jan-Dec) of rainfall (mm/month) in Paramaribo (6°N, 55°W), Natal (6°S, 35°W), Ascension (8°S, 14°W) and San Cristóbal (1°S, 90°W). Multiple year climate data provided by *http://www.weatheronline.co.uk* . Note that the y-axis has different values in each graph.

Fig. 2. **(Top)** Tropospheric ozone (ppbv) at Paramaribo (6°N, 55°W) for the period September 1999 to January 2003, and **(Bottom)** derived seasonality for the whole period based on two week average data. Numbers in parenthesis denote the number of sondes available in each month. The average tropopause height is included as dashed line in the bottom figure.

Fig. 3. Seasonality of ozone (ppbv) as measured from the ozone sondes at **(Top)** Natal (6°S, 35°W), **(Middle)** Ascension (8°S, 14°W), and **(Bottom)** San Cristóbal (1°S, 90°W). Numbers in parenthesis denote the number of sondes available in each month. The average tropopause height is included as dashed line.

Fig. 4. Vertical profiles of ozone (solid) and relative humidity (dashed) for sondes from **(Top)** May, representing the wet season (N=13), **(Middle)** February, representing the short dry season (N=11), and **(Bottom)** September, representing the long dry season (N=19). All available ozone profiles for a given month are displayed in grey, the solid bold line represents the average ozone volume mixing ratio based on these profiles, the dashed bold line is the average relative humidity.

Fig. 5. Composite illustrating the position of the ITCZ over the Atlantic Ocean and the starting point of 5-day backward trajectories. The satellite picture is a water vapor image from METEOSAT for March 31, 2001, while the trajectories (N=17) are from different days, and all end in the boundary layer over Paramaribo. The composite illustrates how the southern position of the ITCZ allows distinctly northern hemispheric air to reach the lower troposphere in Paramaribo during the short dry season.

Fig. 6. Composite illustrating the position of a strong area of subsidence over the Atlantic Ocean, as well as 5-day back trajectories that traverse this region. The satellite image is a water vapor image from GOES-west for March 25, 2001 while the back trajectories are for several different days in March. All trajectories end in Paramaribo between 200-500 hPa, on a descending path. The composite illustrates how upper tropospheric air that is rich in ozone but low in water vapor reaches the middle troposphere over Paramaribo during the short dry season.

Fig. 7. Composite illustrating transport of a plume of biomass burning products from Africa. Arrows denote the 10-day average wind fields at 500 hPa from July 31 to August 9, 2000. Filled circles are locations of fires as observed by the ATSR instrument (Arino and Melinotte, 1995,1998). The insert of Africa shows burning scars from fires observed

from METEOSAT (Pinty, 2000). Contours illustrate the dispersion of a modeled tracer released from the fires into the ECMWF wind fields, and transported to Paramaribo by convection and advection. Widespread ozone enhancements were observed in the Paramaribo ozone profile at August 9, 2000.

Fig. 8. Composite illustrating transport of a plume of biomass burning products from South America. Arrows denote the 3-day average wind fields at 400 hPa from August 28 to August 30, 2000. Filled circles are locations of fires as observed by the ATSR instrument (Arino and Melinotte, 1995, 1998). Contours illustrate the dispersion of a modeled tracer released from the fire locations into the ECMWF wind fields, and transported to Paramaribo by advection and convection. Enhanced ozone VMRs were observed at 400 hPa in the Paramaribo ozone profile on August 30, 2000.

Fig. 9. Seasonality of TTOC as observed in the 1979-1992 NIMBUS-7 TOMS data (Hudson and Thompson, 1998) (dashed line), and based on Paramaribo sondes (1999-2003) (solid line).

Fig. 10. (**Top**) Seasonal cycle of $\Omega_{bck}^{trop}(180^{\circ}\mathrm{W})$ (diamonds and black line) based on an SH ozone sonde climatology (grey line) as given in Hudson and Thompson (1998). (**Middle**) As top, but now with the retrieval based on ozone sondes from Paramaribo (grey line). (**Bottom**) Differences in TTOC from Figure 9 (black solid) can be explained largely from the difference in seasonality of $\Omega_{bck}^{trop}(180^{\circ}\mathrm{W})$ (grey line) in the NH and SH.

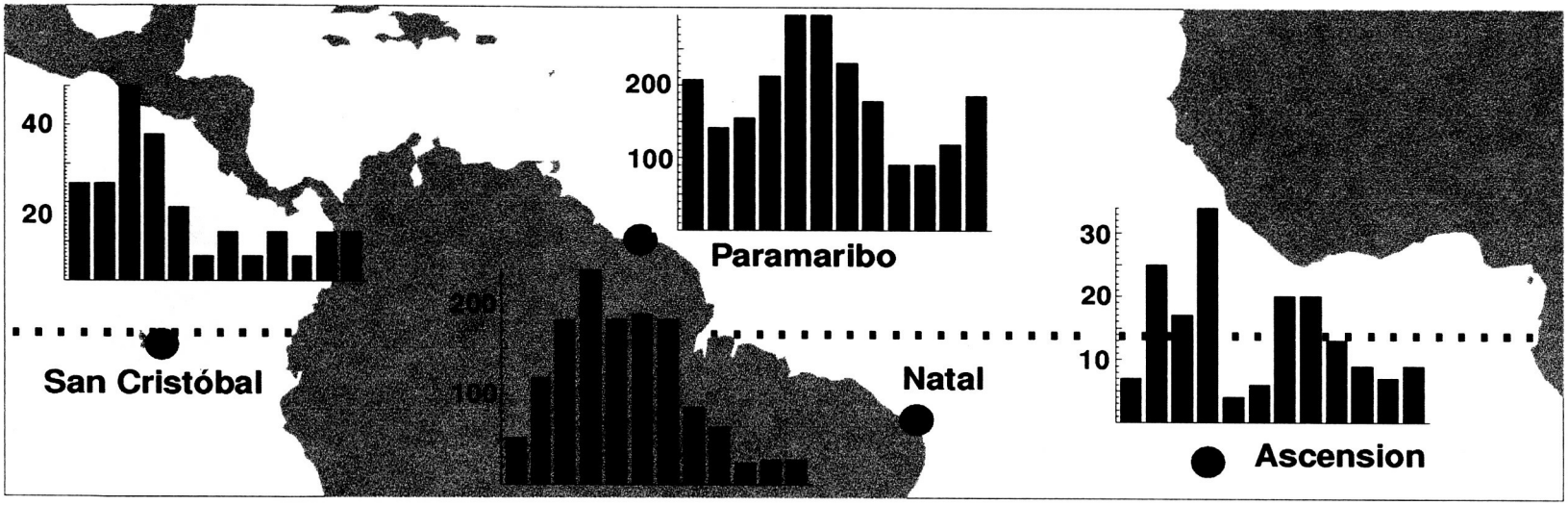

Figure 1: Location and seasonality (Jan-Dec) of rainfall (mm/month) in Paramaribo (6°N, 55°W), Natal (6°S, 35°W), Ascension (8°S, 14°W) and San Cristóbal (1°S, 90°W). Multiple year climate data provided by *http://www.weatheronline.co.uk* . Note that the y-axis has different values in each graph.

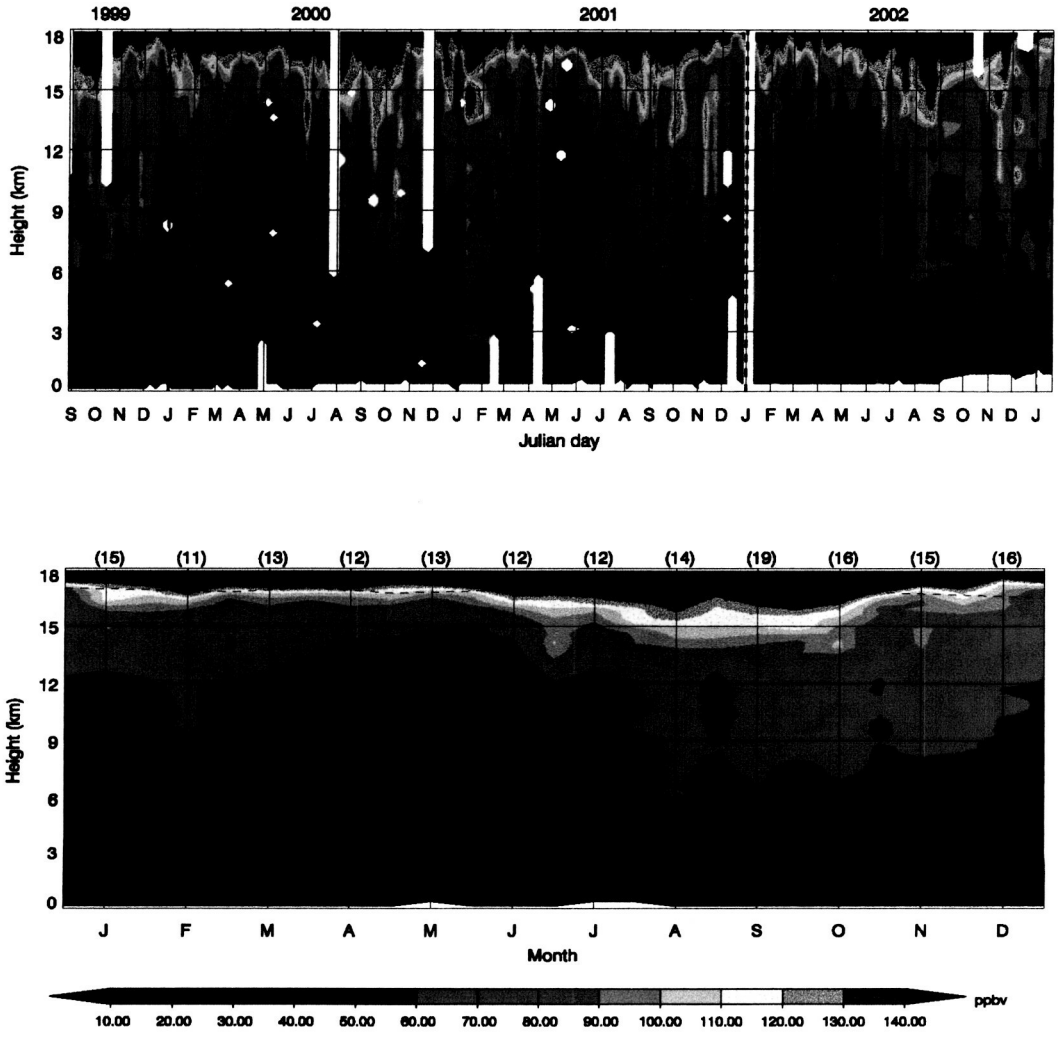

Figure 2: (**top**) Tropospheric ozone (ppbv) at Paramaribo (6°N, 55°W) for the period September 1999 to January 2003, and (**bottom**) derived seasonality for the whole period based on two week average data. Numbers in parenthesis denote the number of sondes available in each month. The average tropopause height is included as dashed line in the bottom figure.

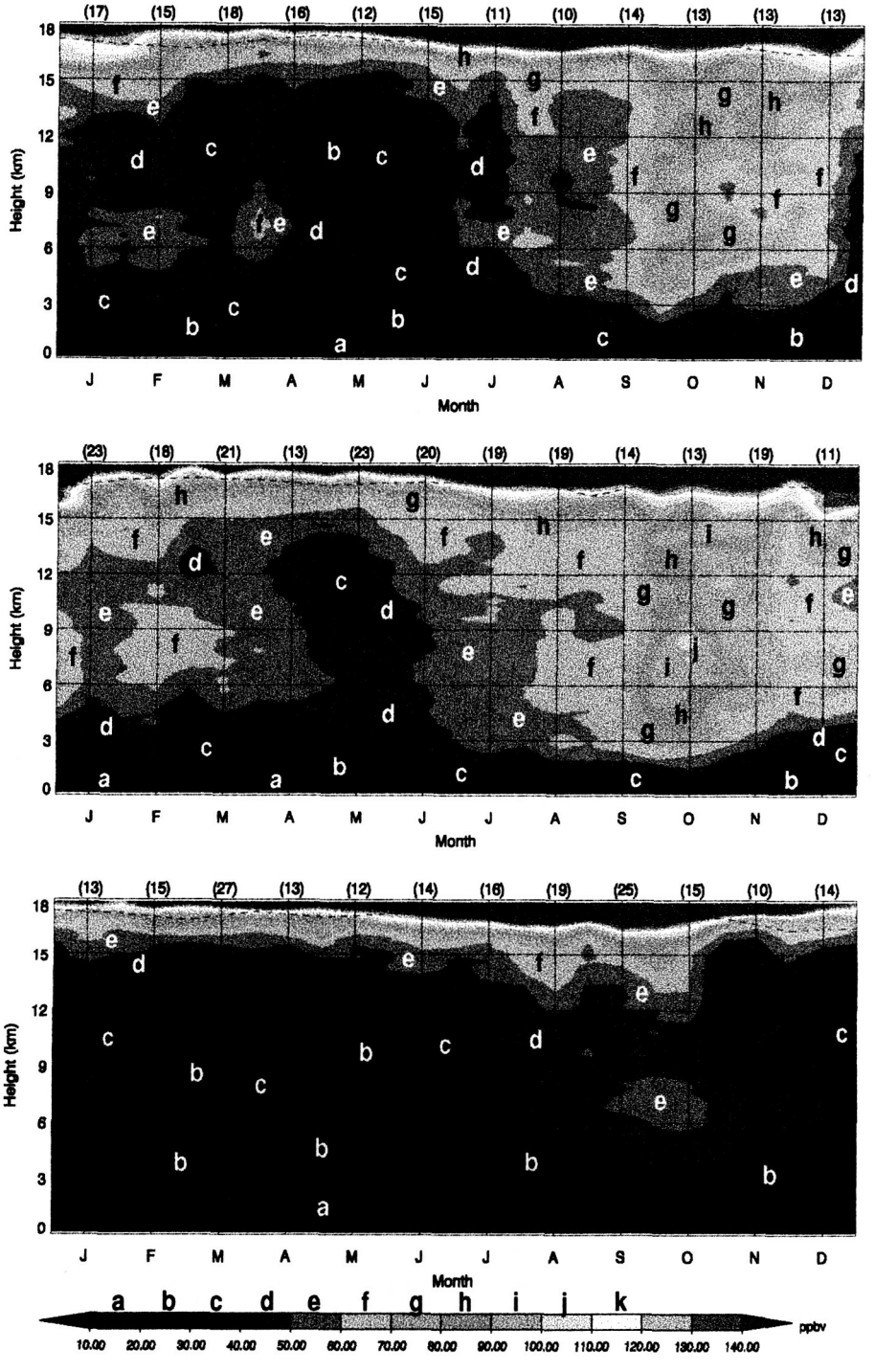

Figure 3: Seasonality of ozone (ppbv) as measured from the ozone sondes at (**top**) Natal (6°S, 35°W), (**middle**) Ascension (8°S, 14°W), and (**bottom**) San Cristóbal (1°S, 90°W). Numbers in parenthesis denote the number of sondes available in each month. The average tropopause height is included as dashed line.

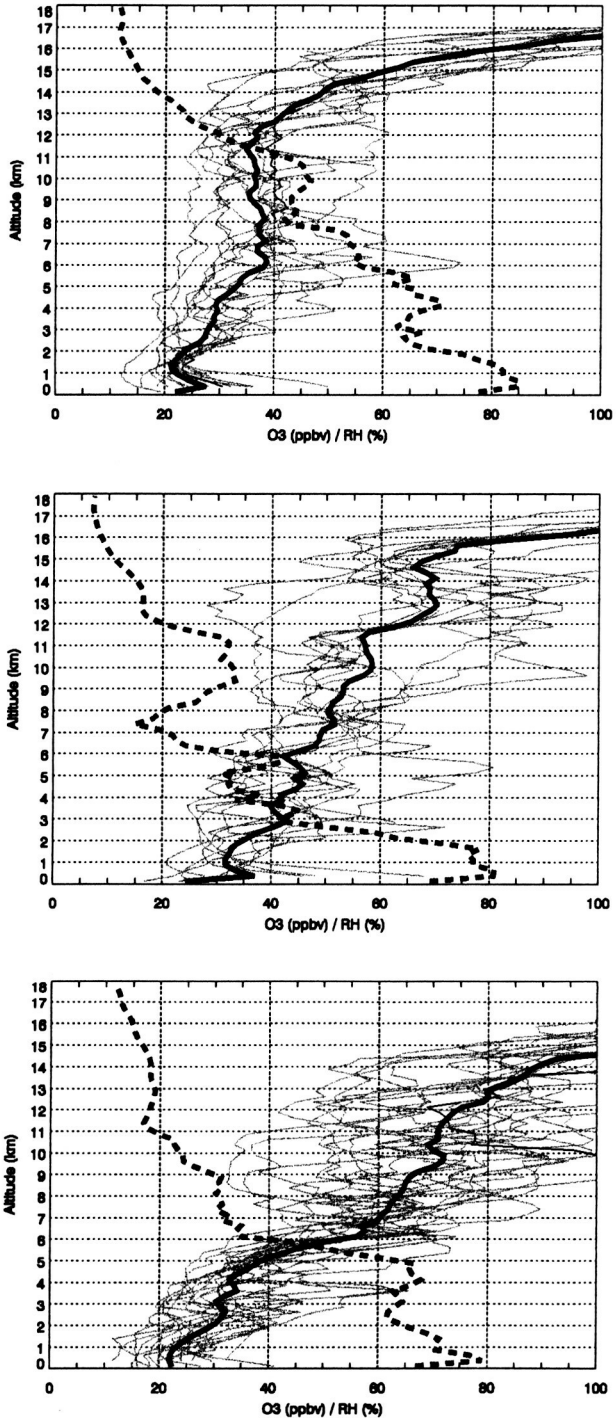

Figure 4: Vertical profiles of ozone (solid) and relative humidity (dashed) for sondes from (**top**) May, representing the wet season (N=13), (**middle**) February, representing the short dry season (N=11), and (**bottom**) September, representing the long dry season (N=19). All available ozone profiles for a given month are displayed in grey, the solid bold line represents the average ozone volume mixing ratio based on these profiles, the dashed bold line is the average relative humidity.

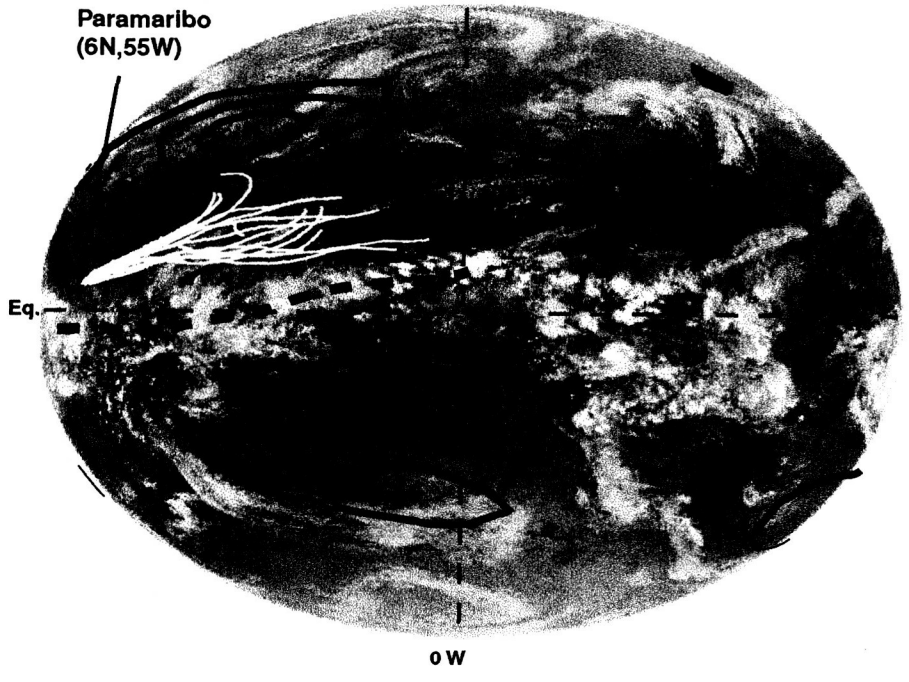

Figure 5: Composite illustrating the position of the ITCZ over the Atlantic Ocean and the starting point of 5-day backward trajectories. The satellite picture is a water vapor image from METEOSAT for March 31, 2000, while the trajectories (N=17) are from different days, and all end in the boundary layer over Paramaribo. The composite illustrates how the southern position of the ITCZ allows distinctly northern hemispheric air to reach the lower troposphere in Paramaribo during the short dry season.

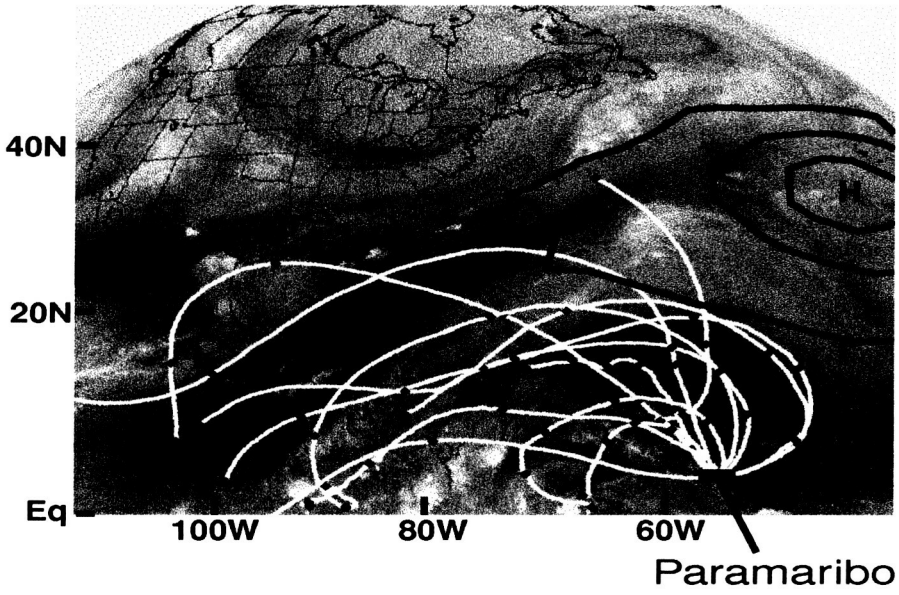

Figure 6: Composite illustrating the position of a strong area of subsidence over the Atlantic Ocean, as well as 5-day back trajectories that traverse this region. The satellite image is a water vapor image from GOES-west for March 25, 2000 while the back trajectories are for several different days in March. All trajectories end in Paramaribo between 200-500 hPa, on a descending path. The composite illustrates how upper tropospheric air that is rich in ozone but low in water vapor reaches the middle troposphere over Paramaribo during the short dry season.

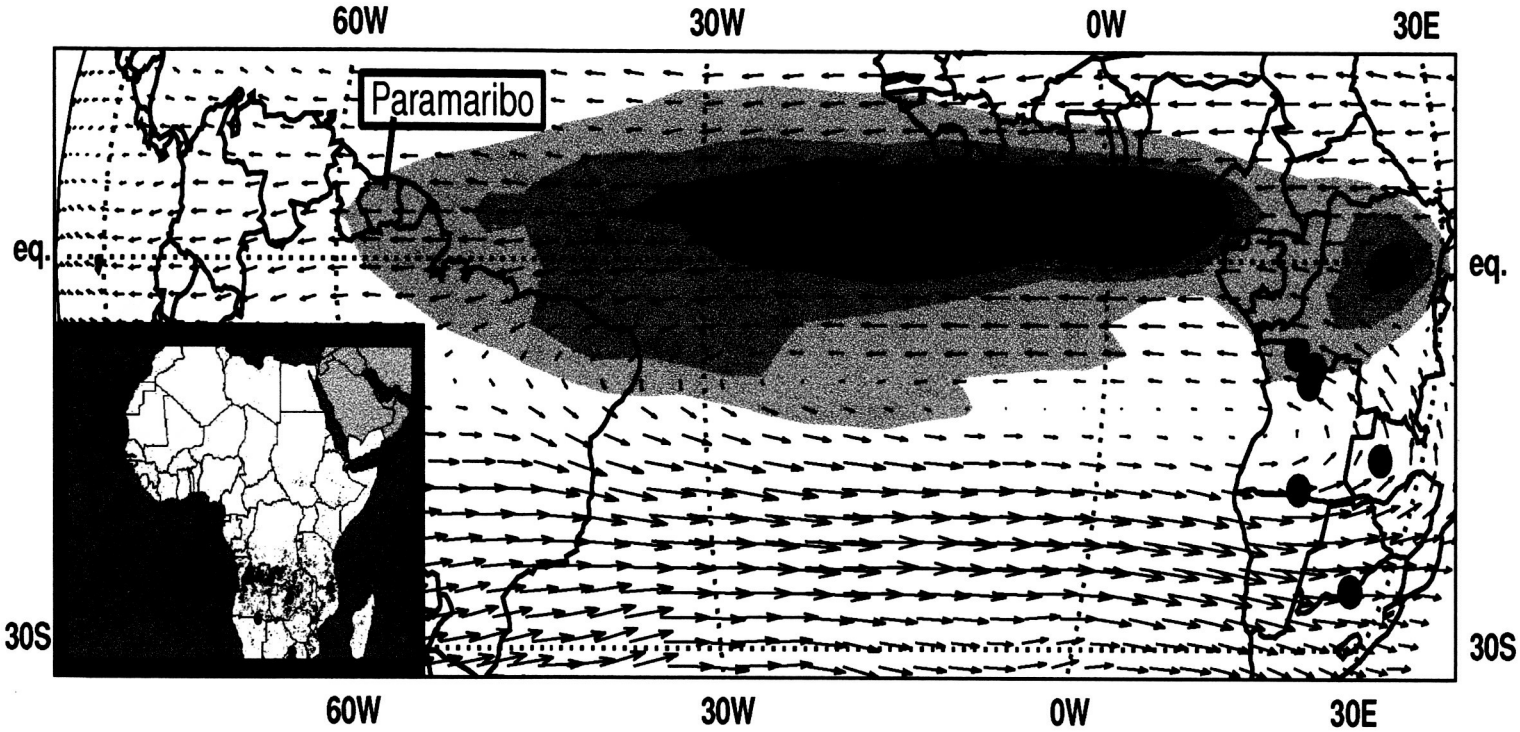

Figure 7: Composite illustrating transport of a plume of biomass burning products from Africa. Arrows denote the 10-day average wind fields at 500 hPa from July 31 to August 9, 2000. Filled circles are locations of fires as observed by the ATSR instrument (Arino and Melinotte, 1995,1998). The insert of Africa shows burning scars from fires observed from METEOSAT (Pinty, 2000). Contours illustrate the dispersion of a modeled tracer released from the fires into the ECMWF wind fields, and transported to Paramaribo by convection and advection. Widespread ozone enhancements were observed in the Paramaribo ozone profile at August 9, 2000.

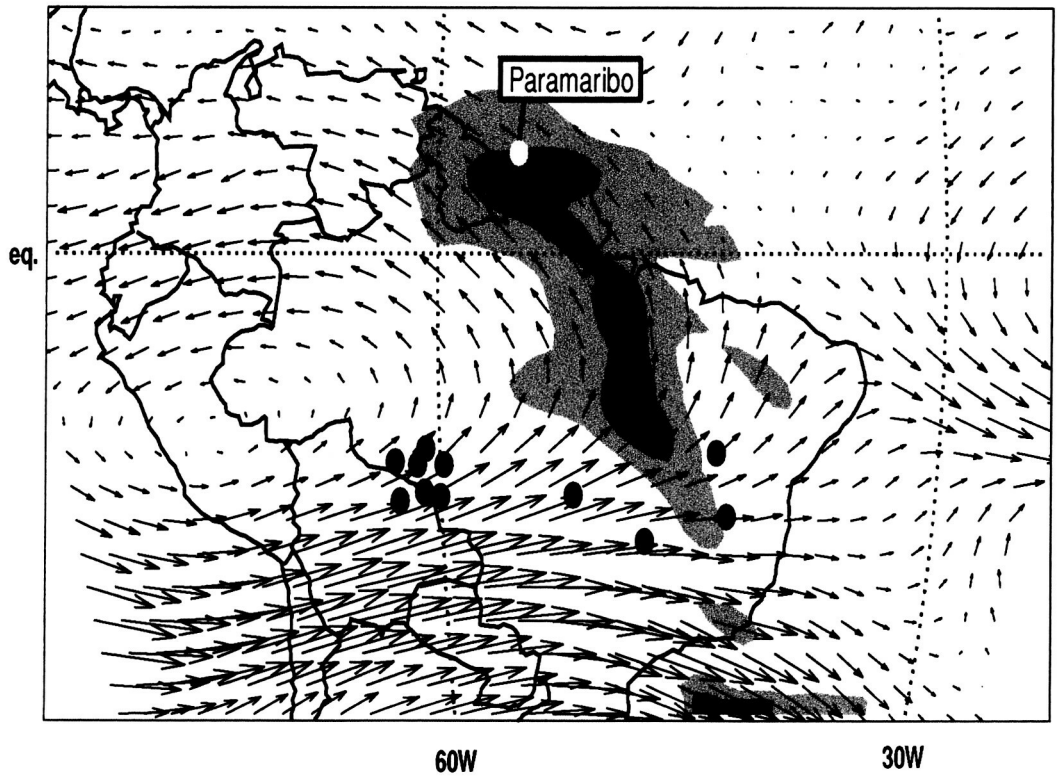

Figure 8: Composite illustrating transport of a plume of biomass burning products from South America. Arrows denote the 3-day average wind fields at 400 hPa from August 28 to August 30, 2000. Filled circles are locations of fires as observed by the ATSR instrument (Arino and Melinotte, 1995, 1998). Contours illustrate the dispersion of a modeled tracer released from the fire locations into the ECMWF wind fields, and transported to Paramaribo by advection and convection. Enhanced ozone VMRs were observed at 400 hPa in the Paramaribo ozone profile on August 30, 2000.

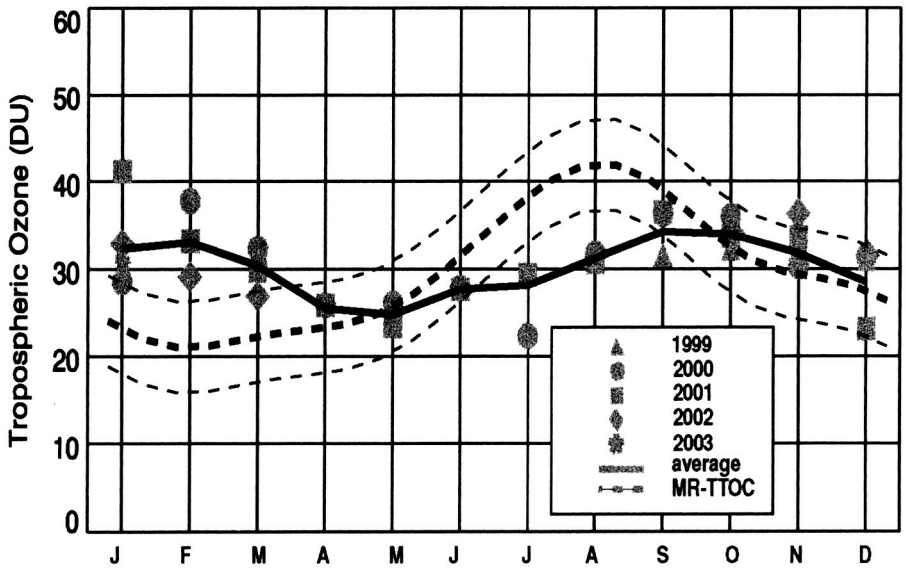

Figure 9: Seasonality of TTOC as observed in the 1979-1992 NIMBUS-7 TOMS data (Hudson and Thompson, 1998) (dashed line), and based on Paramaribo sondes (1999-2003) (solid line).

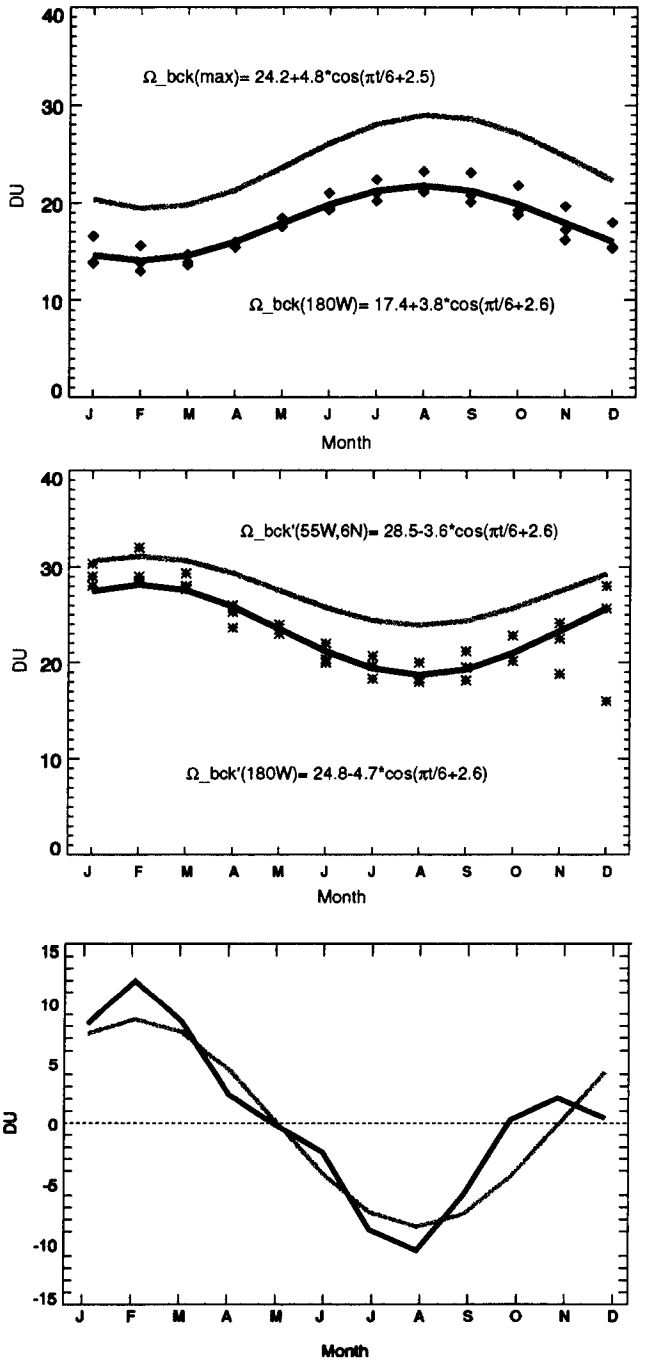

Figure 10: (**Top**) Seasonal cycle of Ω_{bck}^{trop}(180W) (diamonds and black line) based on an SH ozone sonde climatology (grey line) as given in (Hudson and Thompson, 1998). (**Middle**) As top, but now with the retrieval based on ozone sondes from Paramaribo (grey line). (**Bottom**) Differences in TTOC from Figure 9 (black solid) can be explained largely from the difference in seasonality of Ω_{bck}^{trop}(180W) (grey line) in the NH and SH.